

BWR-4 LOCA MODELING WITH RELAP5

K. Nikitin¹, P. Mueller², J. Martin^{2*}, W. van Doesburg², and D. Hiltbrand³

¹: BKW Energie AG, BKW Engineering, Viktoriaplatz 2, CH-3000 Bern, Switzerland

²: BKW Energie AG, NPP Muehleberg, CH-3203 Muehleberg, Switzerland

³: Studsvik, 300 North Third Street, Suite 400, Wilmington, NC 28401, USA

Konstantin.Nikitin@bkw.ch, Pablo.Mueller@bkw.ch, Jimmy.Martin@bkw.ch,
Willem.vanDoesburg@bkw.ch, David.Hiltbrand@studsvik.com

ABSTRACT

A loss of coolant accident (LOCA) is postulated to occur as a break in any of the piping systems connected to the reactor vessel. The break results in the continuous, uncontrolled loss of reactor coolant to containment. Without an adequate source of emergency cooling water, the subsequent fuel heatup could result in fuel damage and the release of fission products from the fuel. Application of best estimate codes and methodologies for LOCA simulation can provide the high level of details of the real plant response necessary to assess the adequacy of an emergency core cooling system. The RELAP5 thermal-hydraulics code was developed for best-estimate transient simulation of light water reactor coolant systems during postulated accidents including LOCA.

Muehleberg NPP (KKM) equipped with a BWR-4 reactor has been using the RELAP5 code from the early 90s for deterministic safety analysis. The current KKM RELAP5 model developed for the KKM plant has been demonstrated to be valid for simulating a wide range of transients including loss of coolant type accidents. Using this model, KKM LOCA analyses have been performed for the recirculation line pump suction break. The simulations have been done for the full break size spectrum. The sensitivity to the most important physics phenomena, e.g. CCFL, and model parameters, e.g. nodalization, has also been assessed.

Results from the KKM RELAP5 LOCA analyses have been compared to the KKM LOCA results obtained with TRACG code by GEH. The plant behavior and PCT results predicted by the RELAP5 model are consistent with those reported by GEH using the TRACG model. The differences observed can firstly be attributed to the diversity in the basic modeling of physical phenomena in the two codes (the TRACG code being one of the most advanced system code currently available for BWRs). In addition, differences may originate from varying details in modeling the KKM plant and core parameters. However, considering that completely independent codes and models of the KKM plant predict similar PCT and plant behaviors during a LOCA, the KKM RELAP5 model can confidently be used to conclude that the GEH TRACG LOCA analysis results are dependable and provide reliable data for comparison against safety criteria.

KEYWORDS

BWR-4, LOCA, RELAP5, cladding temperature, CCFL

1. INTRODUCTION

The requirements of the nuclear safety authorities around the world have been gradually increasing over the last decades. It was mainly caused by a better understanding of the physical phenomena involved in the nuclear energy production, sufficient improvement of modelling tools and demand from the society. This trend strengthened even more after the Fukushima accidents of 2011. Like the rest of the Swiss nuclear power plant operators, BKW, owner and manager of the Muehleberg Nuclear Power Plant (KKM),

* Current affiliation: Institut de Radioprotection et de Sûreté Nucléaire (IRSN), PSN-RES, SEMIA, LIMAR, Cadarache, St Paul-Lez-Durance, 13115, France. Email: jimmy.martin@irsn.fr

invests significant amounts of resources in plant backfittings and further safety improvements of the plant. One of the most important contributors to the KKM safety has been the development of reliable in-house simulation methods and tools.

KKM is a single unit General Electric (GE) boiling water reactor plant with Mark 1 containment that started commercial operation in 1972. Its licensed thermal power output is 1097 MW and its two turbine generator sets produce a net electrical output of 373 MW. The plant is situated on the left bank of the river Aare and forms part of the community of Mühleberg in the Canton of Berne, about 14 km west of the city of Berne.

The first development of an in-house KKM model was completed in the 90s with a second development project starting in 2011 to upgrade the older RELAP5 model to present day modeling methods and current plant design. The second phase of RELAP5 KKM model development was mainly completed in 2014. The comprehensive model validation and verification is described in detail in Reference [1]. Based on the validation results, it is concluded that the RELAP5 KKM model is suitable for simulating a wide class of transients including a loss of coolant accident.

A loss of coolant accident (LOCA) is postulated to occur as a break in any of the piping systems connected to the reactor vessel. The break results in the continuous, uncontrolled loss of reactor coolant to containment. Without an adequate source of emergency cooling water, the subsequent fuel heatup could result in fuel damage and the release of fission products from the fuel. Application of best estimate codes, e.g. RELAP5, and methodologies for LOCA simulation can provide the high level of details of the real plant response necessary to assess the adequacy of an emergency core cooling system. This paper describes the modeling of the full LOCA break spectrum using the RELAP5 in-house model. The model development aspects important for BWR-4 LOCA are also discussed. Finally, the results of RELAP5 LOCA simulation are compared to the results obtained by GEH, KKM fuel vendor, by means of TRACG code.

2. BWR-4 RELAP5 MODEL

The RELAP5 code [2] has been developed for best-estimate transient simulation of light water reactor coolant systems during postulated accidents. The code models the coupled behavior of the reactor coolant system and the core for loss-of-coolant accidents and operational transients such as anticipated transient without scram, loss of offsite power, loss of feedwater, and loss of flow. A generic modeling approach is used that permits simulating a variety of thermal hydraulic systems. Control system and secondary system components are included to permit modeling of plant controls, turbines, condensers, and secondary feedwater systems.

The KKM RELAP5 computer model was developed from documented plant design and performance data. All volumes in the flow path starting at the upper plenum up through the reactor vessel head then down through the upper downcomer and middle downcomer regions are modeled as single flow path volumes with no azimuthal divisions. Radial divisions in these regions are defined based on physical boundaries, e.g., standpipe and separator walls that isolate the separator flow from the upper and middle downcomers. The lower downcomer is split into two azimuthal flow paths based on the recirculation loop connections. Cross-flow is permitted between the two lower downcomer volumes. Two jet pumps are modeled with each representing six individual jet pumps driven by the respective recirculation pump. The jet pumps discharge into the lower head region which is a single flow path volume so any asymmetries in the jet pumps are lost in the lower head as the two flows combine with perfect mixing. The lower head flows into the lower plenum region, another single flow path volume. The lower plenum flow then passes into the core region. The core region is divided into several (from 7 up to 29) fuel channels and a single bypass. More details of the KKM RELAP5 model may be found in Reference [1]. A sketch of a fragment of KKM RELAP5 model is shown in Figure 1. The control systems are based on the real plant algorithms. The control system model includes more than 5000 control elements and variables. Model development is mainly performed using the Symbolic Nuclear Analysis Package (SNAP) [3].

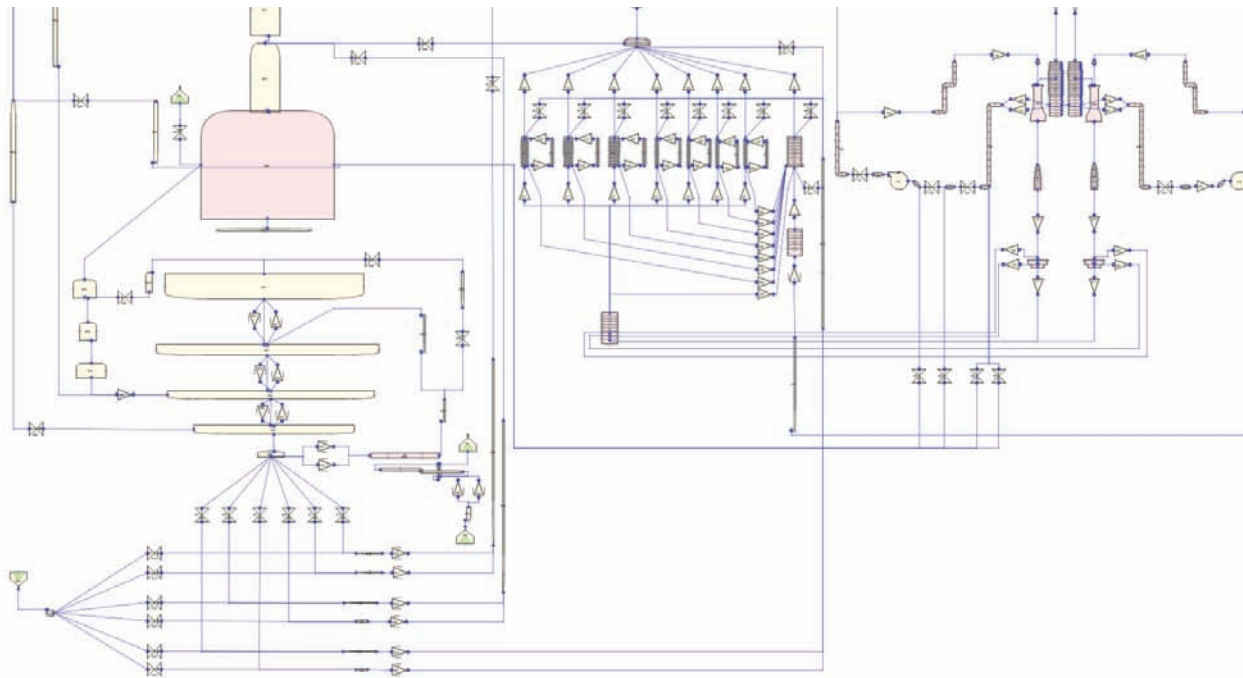


Figure 1. Fragment of KKM RELAP5 model representation.

The KKM RELAP5 model has been validated against plant steady-state and transient operating data, plant test data, and other analyses such as FSAR licensing analyses. Benchmarking to actual plant data demonstrates how well the model simulates the plant response to small and dramatic, planned and unplanned perturbations to steady-state operating conditions, i.e., to plant transients. The transients are initiated by different events and progress at different rates. They exhibit significant changes in reactor power, core flow, recirculation pump speed and flow, feedwater flow and temperature, steam flow, and measured level and a variety of plant control and protection systems are exercised. Successfully benchmarking the model to these transients provides confidence in the fidelity of the model's physics (i.e., the complex interaction between power, vessel pressure, core flow, recirculation pump flow, steam flow, feedwater flow and temperature) as well as the modeled instrumentation and control systems (i.e., level control, pressure control, level measurement, runback logic, and SCRAM logic). More details related to the model validation are given in Reference [1].

3. MODELING ASPECTS IMPORTANT FOR LOCA SIMULATION

Typically, BWR LOCAs are classified based on the break location, break size and available ECCS components. Depending on the variation of these LOCA scenario characteristics, the transient may develop in a completely different manner. The transient response to the LOCA for a BWR-4 is similar to the LOCA response for other jet pump designed BWRs. A good overview of a generic BWR-4 response during LOCA is presented in Reference [4]. The KKM plant behavior during LOCA differs from the generic BWR-4 response mainly due to the specific ECCS configuration/performance. In addition, the KKM reactor power is approximately 3 times smaller than the typical BWR power and the pipe sizing is not fully scalable.

Literature review and preliminary simulations reveal that the following parameters are the most important for KKM LOCA modeling. The importance was defined based on the impact on licensing parameters, e.g.

peak cladding temperature (PCT), local and core-wide oxidation, on the reasonable parameter variations or model modifications.

- Counter Current Flow Limitation modeling,
- Choking flow modeling,
- Downcomer and bypass nodalization,
- Channel grouping,
- Injection flow distribution under low flow rate conditions.

The CCFL modeling approach is described in detail in the following subchapters.

3.1. CCFL phenomenon

The Counter Current Flow Limitation (CCFL) or flooding is one of the key phenomena that govern a BWR's response during the core refill phase of the LOCA. Basically, the ECCS makeup water, which is sprayed into the upper plenum with the intent to fall into the core through the fuel bundle upper tie plates, may be held up by the rising steam flow thereby inhibiting core cooling. Furthermore, during the early stage of a recirculation line break LOCA, the lower plenum water inventory is expected to undergo flashing and hence a substantial steam flow may travel through the core from the lower plenum. Any liquid draining from the core into the lower plenum through the bottom Side Entry Orifices (SEOs) of the fuel bundles may interact with the rising steam flow and be held up in the core thereby benefitting core cooling.

The literature review related to the flooding phenomenon reports two main mechanisms as a possible cause of the CCFL [5]. However, one may note that in spite of more than fifty years of investigations, the CCFL is far from being fully understood and its phenomenology is still an open question for the thermal-hydraulics [6]. The first postulated mechanism relates to wave blockage and is assumed to occur when the channel diameter is less than 50 mm. According to McQuillan and Whalley [7], it can be shown experimentally that from a given gas velocity, the gas flow interacts enough with the falling liquid film to create waves on the interface with the liquid film. These waves will then propagate downwards (i.e. in the direction of the film flow) with a decreasing propagation velocity and a growing amplitude. Possibly, a wave may become stationary at the bottom of the channel. The wave blockage mechanism postulates that when the rising gas velocity is further increased up to a critical value (i.e. corresponding to the onset of flooding), a reversed wave propagation may happen, later accumulating water at the top of the channel and limiting the liquid downflow. If a limiting gas velocity is reached, the overall liquid flows upwards.

The second postulated mechanism refers to droplet entrainment. Given the previous situation of the presence of a stationary liquid wave standing at the bottom of the channel, when a critical gas velocity is reached, droplets are expected to be removed from the edge of the wave and then entrained upwards by the gas flow. Any increase in the gas velocity enhances the dragging of liquid droplets by the gas flow, until a limiting gas velocity is reached, above which the overall liquid flow is prevented from falling down, as seen in Figure 2. Experiments carried out by Zabaras and Dukler [9] showed no evidence of the association of both wave blockage and droplet entrainment phenomena when the onset of flooding is reached. Nonetheless, the droplet entrainment phenomenon is expected to take place from channel diameters exceeding 50 mm and does not show any diameter dependency (whereas droplet entrainment phenomenon does depend on surface tension).

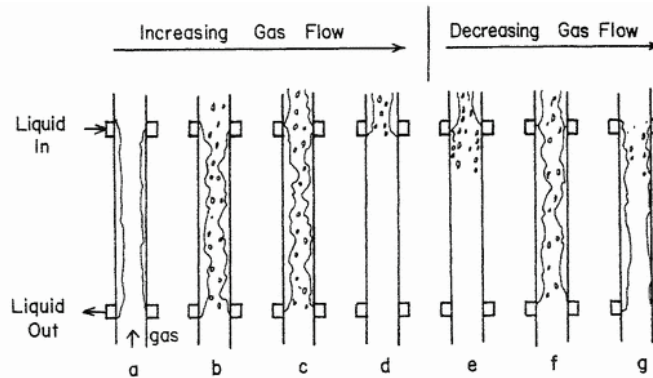


Figure 2. Sketch of the droplet entrainment flooding mechanism from Bankoff et al. [8].

Generally, it has been shown experimentally that the larger is the liquid flow, the smaller is the minimal gas flow from which the onset of flooding is reached [10]. In Figure 3, the pressure gradient above the injection point of liquid within a two-phase flow experimental device (with gas flowing upwards) is illustrated. For a given gas mass flow, a fraction of injected liquid is carried by the gas stream and goes upwards, leading to a pressure drop increase in the upper part of the device. Experimentally, the gas mass flow at which the measured pressure gradient becomes large reveals the flooding occurrence. The gas flow corresponding to the half of the measured maximum pressure gradient is the minimal gas flow required for observing the onset of flooding (for a fixed liquid flow). Nevertheless, it is noted that the CCFL experiments previously cited are purely hydrodynamic and concern the two-phase flow of air and water, not steam and water. Indeed, the air and water flow prevents the mass transfer between both phases and hence, allows studying a given phenomenon through the only point of view of the hydrodynamics. In the case of a LOCA, there is a competing effect in which the maximized ECCS flow leads also to more steam condensation, which tends to reduce the gas flow.

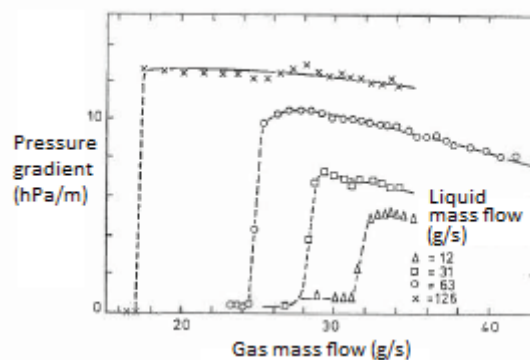


Figure 3. Pressure gradient above the liquid injection point as a function of gas and liquid mass flows [11] (experiments [10]).

3.2. Benchmark of CCFL correlations available within RELAP5

The CCFL phenomenon modeling is implemented within RELAP5mod3.3 through three types of correlations that can be chosen by the user [2]. These correlations are referred to as Wallis, Kutateladze and Bankoff type correlations. The reader may note that the effect of steam condensation on CCFL is not taken into account by the flooding correlations that are presently available within RELAP5. However, all the above correlations are defined by the following equation:

$$H_g^{\frac{1}{2}} + m * H_f^{\frac{1}{2}} = C \quad (1)$$

In this expression, H_f^* and H_g^* are respectively the dimensionless liquid and gas fluxes:

$$H_f = \frac{J_f * \rho_f^{\frac{1}{2}}}{[g * w * (\rho_f - \rho_g)]^{\frac{1}{2}}} \quad (2)$$

$$H_g = \frac{J_g * \rho_g^{\frac{1}{2}}}{[g * w * (\rho_f - \rho_g)]^{\frac{1}{2}}} \quad (3)$$

Where $J_f = \langle \alpha_f * \bar{u}_f \rangle$ and $J_g = \langle \alpha_g * \bar{u}_g \rangle$ are the liquid and gas superficial velocities, α_f and α_g are the liquid and gas void fractions, \bar{u}_f and \bar{u}_g are the time-averaged liquid and gas velocities, g is the gravitational acceleration, ρ_f and ρ_g are the liquid and gas densities. Furthermore:

$$w = D_h^{1-\beta} * L^\beta \quad (4)$$

Where D_h is the hydraulic diameter and L is the Laplace capillary constant, whose expression is (with σ , the surface tension term):

$$L = \frac{\sigma^{\frac{1}{2}}}{[g * (\rho_f - \rho_g)]^{\frac{1}{2}}} \quad (5)$$

The choice of a flooding correlation is taken into account by the code when the user enters a specific value for the β variable that one can find within the single junction card where CCFL is credited:

- A Wallis-type correlation is returned if $\beta = 0$;
- A Kutateladze-type correlation if $\beta = 1.0$;
- A Bankoff-type correlation when $0 < \beta < 1.0$.

This β variable is the one defined by Bankoff et al. [12] and whose expression is later discussed within the present paper. One can note that if $\beta = 0$, one obtains the Wallis dimensionless apparent velocities $H_f = J_f^*$ and $H_g = J_g^*$ whereas if $\beta = 1.0$, one gets the Kutateladze numbers $H_f = Ku_f$ and $H_g = Ku_g$. Likewise, the slope m and the gas-intercept C terms of expression (1) must be entered by the code user.

The below Figure 4, which exhibits the plotting of the dimensionless gas flux as a function of the dimensionless liquid flux according to equation (1), allows interpreting the flooding experiment presented in figure 1. Any point located below one flooding line (let us consider those defined by $C=0.72$) like point (a) in Figure 4, corresponds to a counter-current flow of gas and liquid, where the overall liquid flows downwards. For a fixed inlet liquid flow, an increase of gas velocity leads to intercept the flooding line at point (b). Point (b) represents here the onset of flooding phenomenon. From there, if the liquid entrainment mechanism is credited for instance, the first liquid droplets are carried by the gas stream, and the liquid downflow decreases with any further increase of the gas velocity, from point (b) to point (c). When point (c) is reached, the whole liquid flow is dragged upwards by the gas phase; and the two-phase flow is strictly concurrent. Point (d) corresponds to an increase of gas velocity from point (c). If CCFL is credited, no points above the flooding lines can be reached. However, if the CCFL option is not enabled into the RELAP5 code, one may observe a countercurrent flow of gas and liquid whose dimensionless fluxes calculated using expressions (2) and (3) yield points above the flooding line that one would consider otherwise. In this situation, therefore some upflow of liquid may exist due to entrainment which is to be calculated by the code using its implemented two-phase flow entrainment correlations. However, liquid downflows are allowed at much higher gas upflow velocities than in the case of the occurrence of flooding.

Furthermore, a small value of the gas-intercept C appears more restrictive than a larger one. Indeed, for a given inlet liquid flow, the onset of flooding is reached for a lower gas velocity when the gas-intercept is small, as seen in Figure 4 which exhibits two flooding lines, both with a different gas intercept but a same slope.

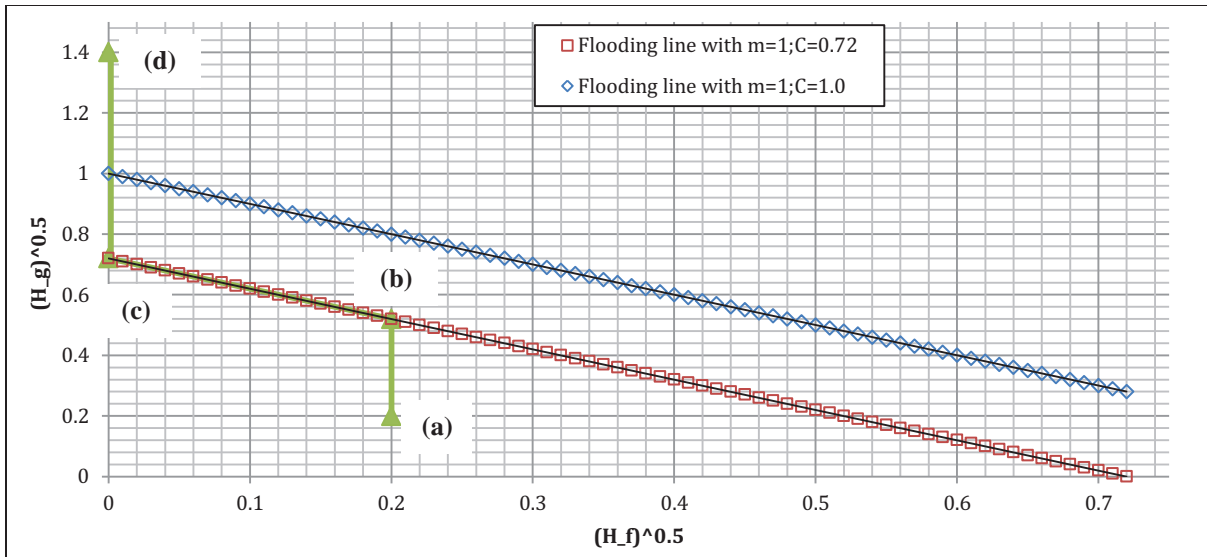


Figure 4. Flooding lines for $m=1$ and $0.72 < C < 1$.

Reference [5] suggests the use of the Wallis correlation that accounts for the flooding mechanism of wave blockage if the geometry where flooding is expected to occur is characterized by a hydraulic diameter of less than 50 mm. Basically, this point corresponds to the fuel bundles upper tie plate geometry whose typical hydraulic diameter is of 10 mm. The Wallis model seems to be suitable for modeling CCFL which may occur at the upper tie plate location, throughout the core reflooding-refill phase of a postulated LOCA [13]. Furthermore, the Wallis correlation is supported by a wide set of experimental data, including the mock-up of a complete BWR pressure vessel (integral effects experiments of [14]). For the particular case of an upper tie plate, Sobajima [15] has shown experimentally the strong dependency of flooding correlations to upper tie plate geometry, i.e. hole size and chamfers, the plate thickness. Hence, Sobajima proposes as well the use of a Wallis-type. Sobajima's proposition is based on a set of steam/water flooding experiments, performed by considering plates of 25 holes (5×5) of 10.5 or 12.0 mm diameter and a pitch of 14.3 mm. Moreover, two different plate thicknesses, i.e. 15.0 and 20.0 mm, and hole chamfer geometries are taken into account [15].

In addition, based on experiments consisting of countercurrent flows of air/water through horizontal perforated plates, [12] proposes the use of a Bankoff-type correlation, where the β term (4) does depend on perforated plate geometry, as follows :

$$\beta = \tanh\left(\frac{2\pi\gamma D_h}{\Delta}\right), \quad (6)$$

where :

- $\Delta \equiv$ thickness of the perforated plate;
- $\gamma \equiv$ perforation ratio = A_{holes}/A_{plate} ;
- $D_h \equiv$ hole hydraulic diameter.

The Bankoff-type correlation is supported by a wide set of experiments which includes perforated plates with 2, 3, 5, 9, 15 or 40 holes with diameters of 4.8, 10.5 or 28.6 mm and a 20 mm plate thickness. Moreover, Bankoff proposes the use of a Bankoff-type correlation with $m = 1.0$ and $C = 2.0$ (for large Bond numbers) since it has been shown that such a flooding model correlates all the air/water experimental data of [12], together with the steam/water experimental data of [16] and [17] for BWR-type full length bundles. When the geometry of the KKM fuel assemblies upper tie plate is considered, this yields $\beta = 0.6$.

Furthermore, for large diameters (i.e. exceeding 50 mm) the reference [18] suggests the use of Kutateladze-like correlations that account for the flooding mechanism of droplet entrainment, which is not diameter-dependent but which does depend on surface tension. Therefore, a Kutateladze-like correlation may be suited for modeling flooding at the fuel bundles Side Entry Orifices (SEOs) located at the bottom of the BWR core. One can note that flooding is postulated to happen at the SEOs location and is not expected at the level of fuel bundles lower tie plate holes, which are located above the SEOs in a typical BWR fuel assembly [14]. In a paper dedicated to the analytical study of flooding for large diameter vertical tubes, Tien [19] suggests that $m = 1.0$ and $C = 1.79$ are used into expression (1) when a Kutateladze-type correlation is considered.

Six different sets of CCFL correlations have been compared, in order to assess the KKM RELAP5 model sensitivity to the flooding modeling. These cases have been gathered into two main sets of simulations – one being "conservative" and another one being "best-estimate". These sets are :

First set (best-estimate) :

- The upper-bounding Wallis-type correlation suggested by Sobajima [15] for the upper tie plates with $m = 0.841$ and $C = 0.423$ and a Kutateladze-type correlation for the SEOs with $m = 1.0$ and $C = 1.79$ (hereafter named as "WallisUp-Kutateladze");
- The lower-bounding Wallis-type correlation suggested by Sobajima [15] for the upper tie plates with $m = 1.0$ and $C = 0.414$ and a Kutateladze-type correlation for the SEOs with $m = 1.0$ and $C = 1.79$ (hereafter named as "WallisLow-Kutateladze");
- The Bankoff correlation for the upper tie plates with $\beta = 0.6$, $m = 1.0$ and $C = 2.0$ and the Kutateladze correlation for the SEOs with $m = 1.0$ and $C = 1.79$ (hereafter named as "Bankoff-Kutateladze").

Second set (conservative) :

- The upper-bounding Wallis-type correlation suggested by Sobajima [15] for the upper tie plates with $m = 0.841$ and $C = 0.423$ and no CCFL correlation for the SEOs (hereafter named as "WallisUp-noCCFL");
- The lower-bounding Wallis-type correlation suggested by Sobajima [15] for the upper tie plates with $m = 1.0$ and $C = 0.414$ no CCFL correlation for the SEOs (hereafter named as "WallisLow-noCCFL");
- The Bankoff correlation for the upper tie plates with $\beta = 0.6$, $m = 1.0$ and $C = 2.0$ and no CCFL correlation for the SEOs (hereafter named as "Bankoff-noCCFL").

A code error in RELAP5 mod3.3 patch05 was also discovered related to the modeling of CCFL at junctions with an abrupt area option of 1 or 2 specified when the junction area is different from the minimum flow area of the connected volumes. This error has been reported to the RELAP5 maintenance organization and they are currently working on a resolution (user problem number UPN-2014-008). The code error occurs when the CCFL inputs are based on the user-defined junction area (which is reasonable for the modeler to do) and the minimum connected volume area is different from the junction area. The code error results in a misuse of the CCFL constants because RELAP5 interprets the CCFL constants to be applicable to a junction with area equal to the minimum flow area of the connected volumes. Thus, if the minimum flow area of the connected junctions is larger than the user-defined junction area, RELAP5 will essentially apply the CCFL model to smaller velocities. This will effectively decrease the strength of the countercurrent flow limiting ability at that junction.

The reader may note that the flooding correlation parameters that are given above correspond to their true values (be these values taken from experimental data or determined from geometrical considerations) and do not account for the mentioned code error for avoiding further confusion. However, prior to any LOCA simulation crediting the occurrence of flooding phenomenon, correction factors have been applied to the corresponding flooding parameters into the KKM model input deck, in order to circumvent this code error. The corresponding corrected parameters are exhibited in Table I.

Table I. Flooding correlation parameters

	<i>M</i>	<i>C</i>	<i>Corr. m</i>	<i>Corr. C</i>	β
Upper-bound Wallis ([15])	0.841	0.423	0.841	0.19	0
Lower-bound Wallis ([15])	1.0	0.414	1.0	0.18	0
Kutateladze ([19])	1.0	1.79	1.0	0.78	1.0
Bankoff ([12])	1.0	2.0	1.0	0.88	0.6

The full break-size spectrum of a recirculation suction line break LOCA has been further considered for comparison of the discussed correlations. The break occurrence coincides with a loss of offsite power. In addition, only one train of Core Spray (CS) is credited throughout the transient. Note, that the unverified developmental input deck has been used for these simulations. The results are not necessarily reflecting the actual KKM conditions. The results obtained with six combinations of flooding correlations and without any CCFL options enabled are shown in Figure 5.

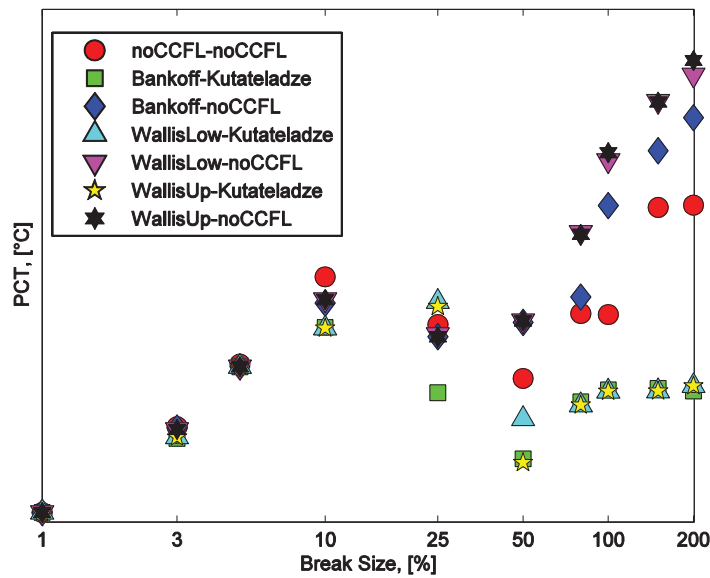


Figure 5. Recirculation suction line LOCA break spectrum with different CCFL correlations.

The above Figure 5 exhibits the importance of the flooding phenomenon that is to take place at the core inlet (i.e. through the Side Entry Orifices (SEOs)). Indeed, one can notice that large PCT differences are obtained when one compares two cases having the same top-core flooding correlation (i.e. Upper-Wallis, Lower-Wallis or Bankoff correlations) but differing only by the presence or absence of a flooding correlation at the core inlet (i.e. Kutateladze or no CCFL models). These differences are observed down to a 10% break size. The first conclusion that can be drawn is that the CCFL is not a key phenomenon of the reflooding-refill phase of a BWR-4 recirculation line LOCA with a break area less than 10% of the suction point area. Furthermore, one can note that Upper-Wallis and Lower-Wallis type correlations from Sobajima [15] applied to the core outlet (i.e. at the upper tie plates location) lead systematically to higher PCTs when compared to the use of a Bankoff-type correlation, each time with no CCFL model credited at the bottom of the core. These differences vanish when the Kutateladze correlation is credited at the core inlet since much smaller temperatures are reached and more generally, when the break size is smaller than 10%. In spite of the care taken by Sobajima [15] in performing air/water flooding experiments and

correlating his data to a Wallis-type correlation, Sobajima's experiment does take into account a limited number of holes, i.e. 25 holes. On the other hand, the Bankoff-type correlation is sustained by a wider set of experimental data, for perforated plates from small to large number of holes (i.e. up to 40 holes) and for a full length BWR-type fuel bundle. Hence it has been decided to use a Bankoff-type correlation for taking into account the occurrence of flooding at the core outlet (i.e. through the upper tie plates). Moreover, it has been shown that the flooding that is to take place at the core inlet is of considerable importance since it leads to wide PCT differences when it is taken into account or not. The consulted thermal-hydraulics literature does not refer to SEO flooding in the same extent than to perforated plate or simple vertical tube flooding or even than to the flooding of a horizontal leg of a PWR under LOCA conditions. However, for large orifices exceeding 50 mm, the literature recommends the use of a Kutateladze-type correlation. It may be difficult to adjust Kutateladze parameters to the SEO geometry with accuracy (which is not a simple vertical tube with an inlet orifice exceeding 50 mm but which is an inclined orifice) and it has been decided to remove any flooding correlation from the core inlet model. One can notice that this choice leads also to more conservatism in the case of core inlet flooding for the full break spectrum (cf. Figure 5).

3.3. Physical/numerical instability issues for BWR-4 RELAP5 model

During the model development a very strong sensitivity to small model perturbations was observed for some transients. The considered small perturbations include variations of maximal time step (from 0.01 s to 0.0001 s), variations of break flow area for LOCA (from -0.5% to +0.5%), variations of modeling parameters, e.g. for choking flow, small variations of the initial conditions, etc. The performed simulations showed that the time step variation covers well all the other types of perturbations. In order to filter the simulation cases where the physical/numerical instability may occur, all the cases with BWR-4 RELAP5 model are being performed with at least 8 different time steps. It means that to generate Figure 5 as many as 560 runs ($10 \times 7 \times 8$) were necessary to perform. When the PCT scatter is not large the maximal among 8 runs PCT is taken as a final value. Some cases are run with 15 different time steps what brings 90% coverage and 80% confidence according to a non-parametric statistics methodology.

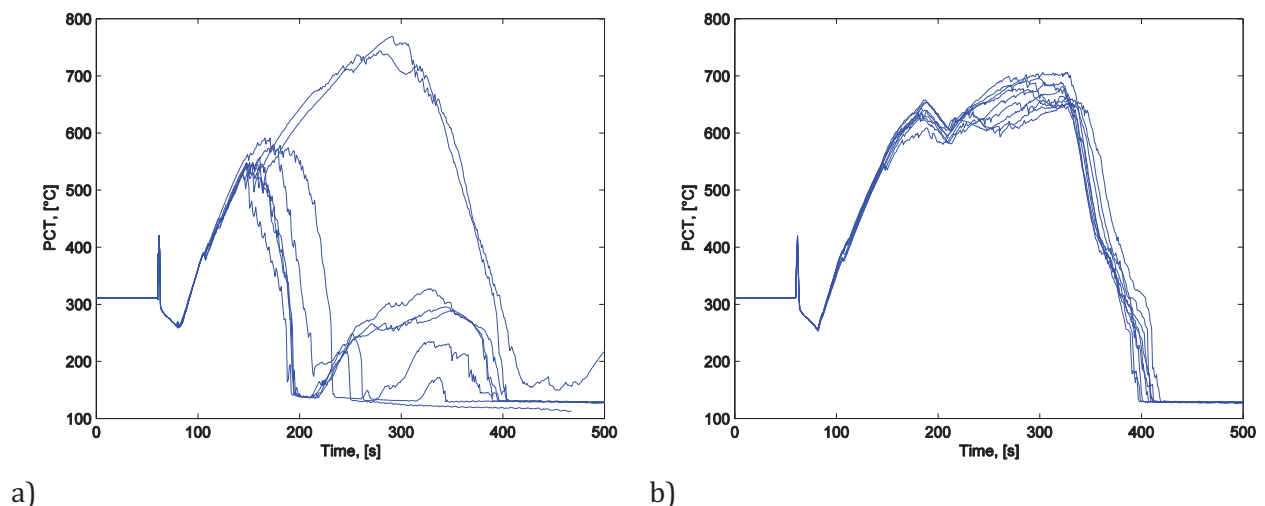


Figure 6. Recirculation suction line break with 1 CS failure for different time steps, a) PCT before model modifications, b) PCT after model modifications.

At the early stage of the model development the physical/numerical instability often occurred as a result of amplification of several misapplications of the best modeling practice. Figure 6a illustrates how much the PCT may fluctuate for different time steps for the double-ended guillotine break of recirculation

suction line. The PCT scatter is as high as 300°C. The model sensitivity analysis showed that two modeling aspects are primary responsible for such a high PCT scatter, i.e. the modeling of the choking flow and the modeling features of the piping connecting the torus and the drywell. Initially, the choking flow modeling has been activated in too many locations, e.g. almost all locations of the channels. It was fixed by initialization of the choking flow modeling flag only in the location where choking phenomena may really occur. The modeling of the piping connecting the torus and the drywell has been refined by renodalization. These two modifications drastically improve the simulation results. The PCT scatter was reduced to approx. 80°C (Figure 6b). Note, that for many transients these model changes don't affect the results at all. The results presented in Chapter 3.2 are obtained with the modified model.

4. RESULTS OF LOCA SIMULATIONS

4.1. 200% recirculation line break with 1 CS failure

After the extensive and intensive KKM RELAP5 model validation/verification [1] the different scenarios of LOCA have been simulated. Special attention has been paid to the system interactions, specific setpoints (and to setpoints sensitivities) and plant-specific ECCS behavior. The following main assumptions were applied.

- A full core of GNF2 fuel assemblies is assumed.
- When more than one initiating signal for a safety function is available, the second/delayed signal is used.
- Loss of external power is assumed at the most unfavorable point in time.
- The most limiting single failure and break size location is assumed.
- The decay heat curve according to ANS-5.1/1979 is used.
- No credit is taken for the feedwater coolant injection system.

Some selected results for a 200% recirculation line break are presented below.

A break is simulated in one of the recirculation lines at the suction of the recirculation pump. The 200% break is modeled as a double-ended guillotine break. For the double-ended guillotine break, two valves (LOCA valves), each with a full-open area equal to the recirculation pipe area and connecting the recirculation piping to the drywell, are fully opened to simulate the break. A third valve (LOCA isolation valve) is modeled as a dummy junction internal to the recirculation pipe and is closed to prevent any communication between the two postulated broken pipe ends. The ECCS available to mitigate the accident includes 2 trains of Reactor Core Isolation Cooling (RCIC), one train of CS, and 2 trains of Alternate Low Pressure Spray (ALPS).

A large BWR LOCA can be described as progressing through three main phases: blowdown, lower plenum flashing, and refill/reflood. A detailed description of each phase may be found in References [21], [22] and [4]. Figure 7 a)-d) show the main results for 200% recirculation line break. During the first seconds, the vessel begins to depressurize rapidly (Figure 7a). The break flow peaks around 6000-8000 kg/s. The downcomer level, lower plenum liquid level and fuel channels liquid levels decrease rapidly. The downcomer level reaches quickly Level 2 setpoint and soon the ECCS, except the unavailable 1 CS train, starts water injection (Figure 7b). At approx. 120s the total ECCS flow exceeds the break flow (Figure 7c). It results in all the levels recovery. The PCT growth is suppressed by the increasing water level at approx. 230 s at the level below 800°C.

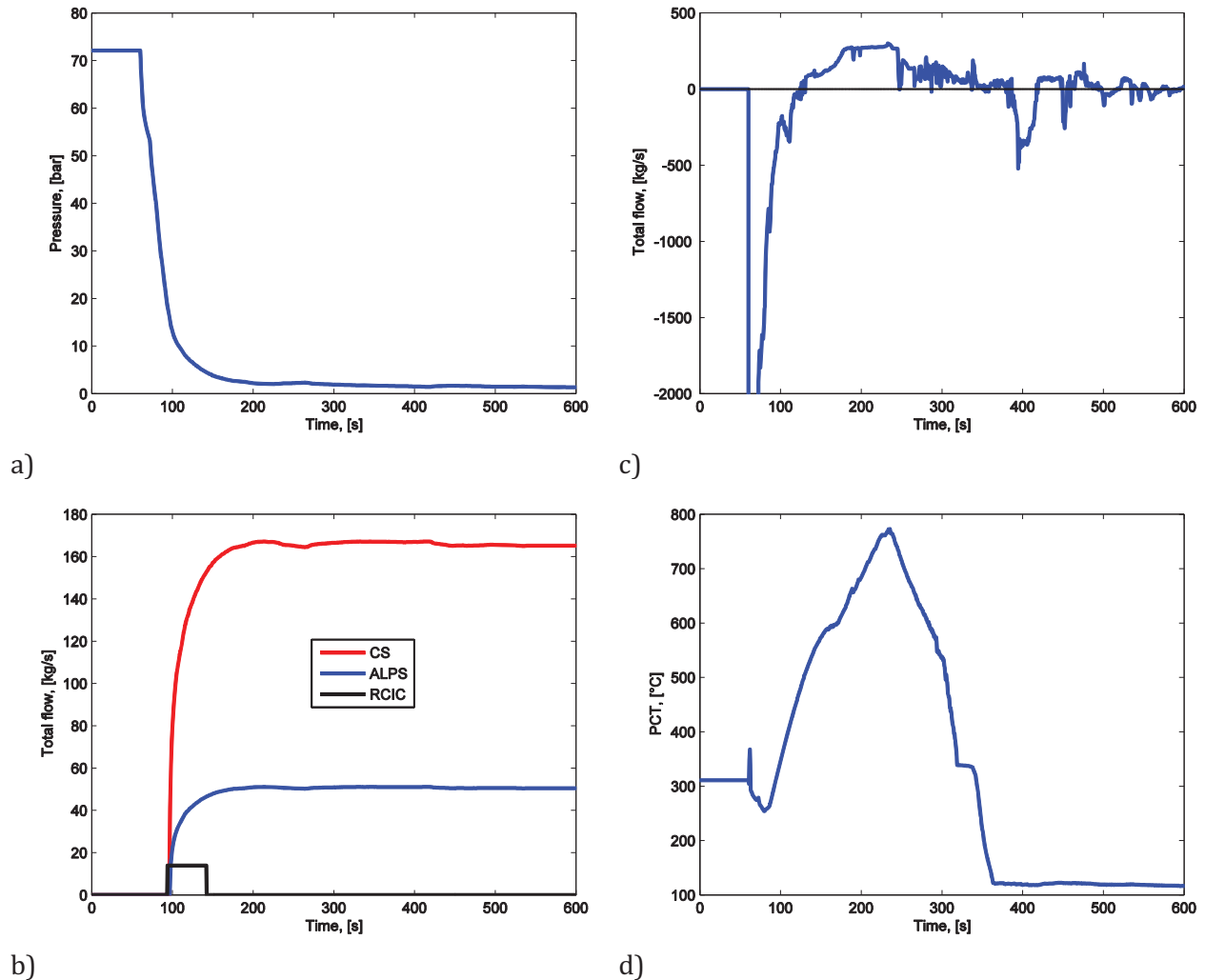


Figure 7. Recirculation suction line break with 1 CS failure, a) dome pressure, b) ECCS flows, c) difference between the break flow and the ECCS flows, c) PCT.

4.2. Comparison with TRACG licensing simulations

The KKM fuel supplier, General Electric - Hitachi Nuclear Energy (GEH), performed a licensing KKM LOCA analysis during 2014-2015 using TRACG code. TRACG is a state-of-the-art tool for the analysis of BWR (two phase flow) transients and accidents [23]. Its development started during the 1980's, mainly for benchmarking and verification of tools used for safety analysis applications at that time, and was further developed in particular for the analysis of new reactor types (SBWR, ESBWR) during the 1990's and beyond. TRACG includes a detailed and realistic (best-estimate) modeling of the physical phenomena during BWR transients, and is currently one of the most advanced modeling tools for analyzing BWR transient behavior.

In order to perform an independent verification of GEH LOCA analysis, the recirculation suction line break data were compared with the results obtained with KKM RELAP5 model. Note, that some parameters of the KKM RELAP5 model were adjusted to be close to the TRACG model. For example, the TRACG top-, middle-, and bottom-peaked power profiles were adopted. Cases representing a spectrum of break sizes ranging from the smallest break of 1% of the flow area of the recirculation pump suction piping up to a double-ended guillotine break or 200% of the flow area of the recirculation pump

suction piping are run. The 200% break modeling technique is described in Section 4.1. For all other break sizes, the two ‘LOCA valves’ open to one-half of the desired break area each and the ‘LOCA isolation valve’ remains fully open.

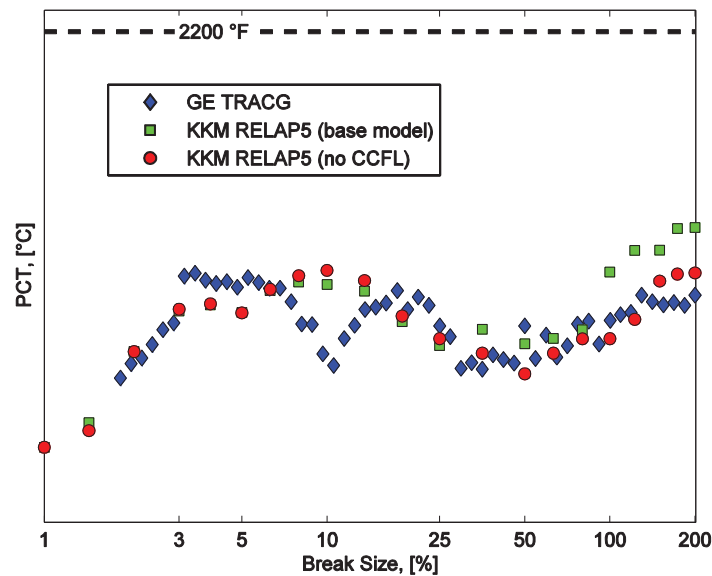


Figure 8. Comparison of TRACG and RELAP5 results for the recirculation line break spectrum.

The result of comparison is presented in Figure 8. The maximum values of the cases with ADS and CS single failure are shown. In general, there is a good agreement between TRACG and RELAP5 results. Some differences are observed in the vicinity of the 10% break where the TRACG results are lower. For 100-200% breaks the RELAP5 PCT is visibly higher. Possible reasons for such dissimilarity are the dissimilar choking models and the differences in CCFL modeling. Without any special CCFL model applied the RELAP5 results are quite close to the TRACG data except for 8-12% breaks.

5. CONCLUSIONS

A RELAP5 BWR-4 model has been developed, validated and applied for LOCA analysis. Using this model, KKM LOCA analyses have been performed for the recirculation line pump suction break. The simulations have been done for the full break spectrum. The sensitivity to the most important physics phenomena, e.g. CCFL, and the model parameters, e.g. nodalization, has also been assessed. The results have been compared to the KKM LOCA results obtained with TRACG code. The plant behavior and PCT results predicted by the RELAP5 model are consistent with those reported by GEH using the TRACG model. The observed differences can firstly be attributed to the diversity in the basic modeling of physical phenomena in the two codes. In addition, differences may originate from varying details in modeling the KKM plant and core parameters. However, considering that completely independent codes and models of the KKM plant predict similar PCT and plant behaviors during a LOCA, the KKM RELAP5 model can confidently be used to conclude that the GEH TRACG LOCA analysis results are dependable and provide reliable data for comparison against safety criteria.

REFERENCES

1. P. Mueller, K. Nikitin, W. van Doesburg, and D. Hiltbrand, “RELAP5 BWR-4 model validation for NPP Mühleberg (KKM),” *Proceedings of NURETH-16*, Chicago, IL, USA, August 30-September 4, 2015, paper 13289, (2015).

2. RELAP5/MOD3.3 Code Manual, NUREG/CR-5535 Rev P4, Volumes 1 through 8, October (2010).
3. Symbolic Nuclear Analysis Package (SNAP), <https://www.nrcsnap.com/snap/>, (2015).
4. J.G.M. Andersen, et. al., "Realistic Assessment of Break Size in Simulated BWR Loss-of-Coolant Accidents," *Proceedings of NURETH-13*, Kanazawa City, Ishikawa Prefecture, Japan, September 27-October 2, Paper N12P1251, (2009).
5. J. Palen, Z.H. Yang, "Reflux condensation flooding prediction: review of current status," *Institution of Chemical Engineers*, **Vol. 79**, Part A, (2001).
6. J.R.F. Guedes de Carvalho, M.A.R. Talaia, *Interfacial shear stress as a criterion for flooding in counter current film flow along vertical surfaces*,"*Chemical Engineering Science*, **Vol. 53**(11), p.2041-2051, (1998).
7. K.W. McQuillan, P.B. Whalley, G.F. Hewitt, *Flooding in vertical two-phase flow*, *International Journal of Multiphase Flow*", **Vol. 11**(6), p.741-760, (1985).
8. S.G. Bankoff *et al.*, *A critical review of the flooding literature*,"*Multiphase Science and Technology*, p.95-180, (1986).
9. G.J. Zabaras, A.E. Dukler, *Counter-current gas-liquid annular flow including the flooding state*," *AIChE J*, **Vol. 34**, p.389-396, (1988).
10. A.E. Dukler, L. Smith, *Two-phase interactions in countercurrent flow. Studies of the flooding mechanism*,"US NRC Contract AT (49-24) 0194, Summary report No 1., (1976).
11. J.M. Delhaye, *Thermohydraulique des Réacteurs*, Collection Génie Atomique, EDP Sciences, (2008).
12. S.G. Bankoff, R.S. Tankin, M.C. Yuen, C.L. Hsien, *Countercurrent flow of air/water and steam/water through a horizontal perforated plate*,"*International Journal of Heat and Mass Transfer*, **Vol. 24**(8), p.1381-1395, (1981).
13. F.J. Moody, R.T. Lahey, *The Thermal-Hydraulics of a Boiling Water Nuclear Reactor*, American Nuclear Society, (1977).
14. H. Nagasaka et al., *Thermal Hydraulic Behavior in Upper Plenum during Refill-Reflood Phase of BWR LOCA*,"*Journal of Nuclear Science and Technology*, **Vol. 22**, p.903-914, (1985).
15. M. Sobajima, *Experimental Modeling of Steam-Water countercurrent Flow Limit for Perforated Plates*,"*Journal of Nuclear Science and Technology*, **Vol. 22**, p.723-732, (1985).
16. M. Naitoh, K. Chino, R. Kawabe, *Restrictive effect of ascending steam on falling water during top spray emergency core cooling*,"*Journal of Nuclear Science and Technology*, **Vol. 15**, p.806, (1978).
17. D.D. Jones, *Test report: TLTA components CCFL tests*, General Electric Company, NEDG-NUREG-23732, (1977).
18. G.F. Hewitt, *In Search of Two-Phase Flow*, Max Jakob Award Lecture, 30th National Heat Transfer Conference, Portland (USA), (1995).
19. D.L. Tien, *A simple analytical model for counter-current flow limiting phenomena with vapor condensation*,"*Letters in Heat and Mass Transfer*, **Vol. 4**, p.231-238, (1977).
20. Anforderungen an die deterministische Störfallanalyse für Kernanlagen: Umfang, Methodik und Randbedingungen der technischen Störfallanalyse (Requirements on the deterministic accident analysis for nuclear installations: scope, methodology and boundary conditions of the technical accident analysis), Guideline ENSI-A01, (2009).
21. E. Hill, *Compendium of ECCS (Emergency Core Cooling Systems) Research for Realistic LOCA (Loss-of-Coolant Accidents) Analysis*, NUREG-1230, NRC, (1988).
22. U.S. Rohatgi, P. Saha, V.K. Chexal, *Considerations for Realistic ECCS Evaluation Methodology for LWRs*, BNL-NUREG-37036, (1985).
23. TRACG Model Description, GEH Licensing Topical Report, NEDO-32176, Revision 4, Non-Proprietary Version, (2008).
24. TRACG Qualification, GEH Licensing Topical Report, NEDO-32177P, Revision 3, Non-Proprietary Version, (2007).